Supplementary Material for A flight-first approach for contrail detection using ground-based cameras

S1 Summary of historic ground-based observations of contrails

Table S1: Summary of historic ground-based observations of contrails.

Study	Source & Size of Dataset	Method/Model	Performance Metrics	Contrail Classification
Schumann et al. (2013)	Multi-camera system; 4 contrails	Manual comparison (flight track)	- [proof of concept]	None
Rosenow et al. (2023)	Multi-camera system; 1778 contrails over 66 days	Manual comparison (flight track)	- [validation of contrail lifecycle model]	None
Low et al. (2024)	Single camera; 281 flights across 14 hours	Visual inspection (CoCiP)	- [CoCiP validation]	Short-lived, intermediate, persistent
Pertino et al. (2024)	All Sky camera; 1,786 visible images and 1,694 infrared images.	YOLOv9c (visible and IR)	mAP@0.5 = 0.739 (visible), 0.591 (IR)	None.
Gourge et al. (2025)	Fish-eye lens; 1,600 images.	Manual segmentation using projected flightpaths using the Roboflow platform.	Dataset creation.	Estimated into young, old, and very old.
Huffel et al. (2025)	USB webcams; 5,016 images.	YOLO1x-seg; Enhanced Mask R-CNN	Yolo11x-seg mAP@0.5 = 0.650; Mask R-CNN mAP@0.5= 0.566	Estimated into short, thin, wide, and cirrus.
Jarry et al. (2025)	All Sky camera; Video dataset of 4,651 contrails with 3,346 being flight matched.	Mask2Former (Swin-L)	AP@[0.25:0.75] = 0.37 (images), 0.34 (video)	None.

Performance is reported using Average Precision (AP), which is the area under the precision-recall curve over different Intersection over Union (IoU) thresholds. For example, the mAP@0.5 measures average precision where a prediction is considered as positive if the area of overlap between the predicted and ground truth region is at least 0.5 of their area of union, AP@[0.25:0.75] reports the average precision across IoUs from 0.25 to 0.75.

S2 Regarding SAM2

Unlike convolutional models that take many layers to build up scene understanding, SAM2's Vision Transformer based architecture processes images globally with a self-attention mechanism. This makes it particularly fit for detecting elongated and dispersed structures like contrails. Furthermore, contrails form and evolve dynamically, often appearing faint, disjointed, or partially obscured, and can disperse irregularly, break apart, grow in width, or fade away, all of which is behaviour that differs heavily from SAM2's training data consisting of strong object presence and continuity.

S3 Regarding contrails advecting out of the field of view before they can be classified

The global 99th percentile wind speed at an altitude of 12 km is 60 ms^{-1}, which corresponds to fast jet stream strength wind (Hersbach et al. 2020). This would result in an advected distance of 7.2 km over the 120 second threshold used to classify short-lived contrail classification threshold. The FOV footprint mapped at 12 km is trapezoidal with sides of 31.6 km, 14.0 km, 21.2 km, and 18.3 km. Under a conservative and extreme case scenario in which the 99th percentile strength wind field is perfectly perpendicular to the shortest side of the FOV, and contrails form orientated parallel to this boundary, a contrail could advect a distance equivalent to 51% of the shortest boundary within two minutes before advecting out of the FOV. This suggests that while persistent contrails could advect out of the FOV before being classified, such cases would require perfectly aligned extreme winds and aligned flight paths.

S4 Classification model performance

S4.1 Formation contrails

The features from masks corresponding to 2,395 directly intersecting flights were selected for training and testing the RFM for formation contrails (intermediate/persistent only). Confusion matrices for both the full dataset and test subset, showing the precision and recall for both contrails and spurious detections, illustrate the classification performance of the RFM in distinguishing between masks left by genuine contrails versus spurious detections (Fig. 5). We find that strong performance is retained on the test-subset of flights, indicating at the model's robustness.

To evaluate the feature importance that different metrics derived for classification had within the RFM decision making, we use the Mean Decrease in Impurity (MDI) method (Han, Guo, and Yu, 2016; see Fig. A1):

- The most influential feature was mask size, reflecting that genuine contrails typically yield a consistent mask area. This is likely due to their progenitor flights usually being at similar altitudes and hence distances away from the camera. This also demonstrates the importance of the individual mask cleaning process to remove unrelated detections that artificially expand the mask area.
- The SAM2 confidence score was the second most influential feature as well-defined features in the scene lead to higher confidence segmentations. Such a feature being influential is perhaps expected, although it being only the second most influential feature in the flight-first approach is itself noteworthy; in detection-first approaches, model confidence in object segmentation is primary, making it the most relied upon task and hence a potentially key failure point.
- The ratio of empty masks also emerged as a highly influential feature, further demonstrating the importance of a robust mask cleaning process. As each frame is cleaned independently, frames that yield no valid features within the padded flight path envelope are filtered out. This allows the ratio to serve as an informative feature. The importance

of this feature highlights that flights without a contrail are characterised by frequently empty or invalid masks (a pattern that would not be as clearly measurable without the flight-first approach or individual mask cleaning step).

- The expectance of a spatially and texturally coherent contrail is highlighted through the indicated importance of the mean width and its standard deviation. The standard deviation of the mask pixel intensity was thus also amongst the most influential features.

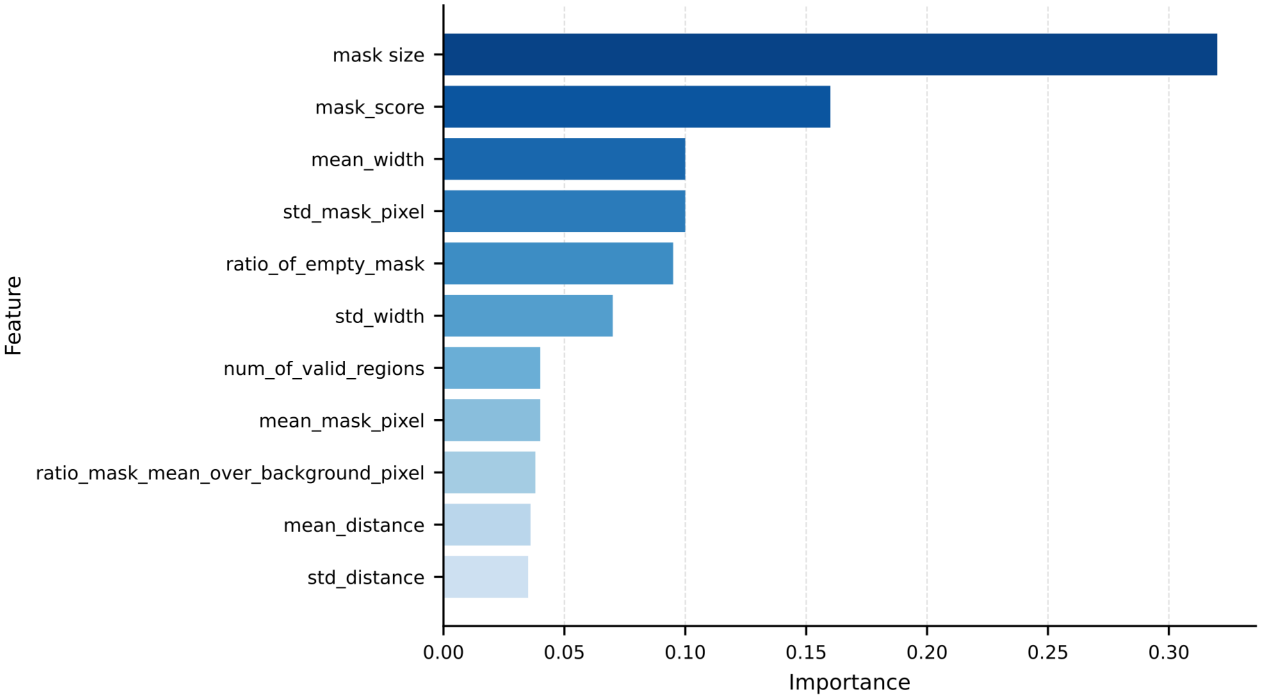

Figure S1: Feature importance for the formation RF model based on the Mean Decrease in Impurity. Importance is sum-to-one normalised, thus effectively showing relative importance of different features.

S5 Further case studies of segmentations and detections

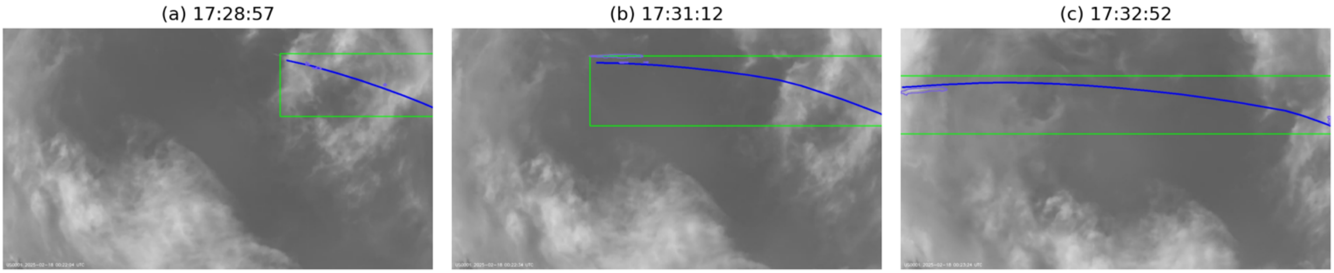

Figure S2: The overlaid masks from a short-lived and rapidly dissipating contrail segmented successfully. The contrail only extends a small distance behind the aircraft. The advected flightpath is drawn in blue, the input box is in green, and the mask is contoured in purple.

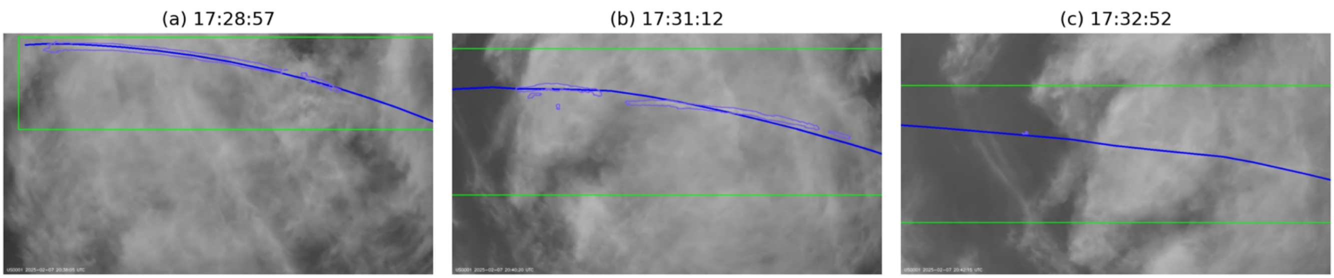

Figure S3: The overlaid masks from a short-lived contrail segmented successfully. The contrail fully extended behind the aircraft before it dissipates. The advected flightpath is drawn in blue, the input box is in green, and the mask is contoured in purple.

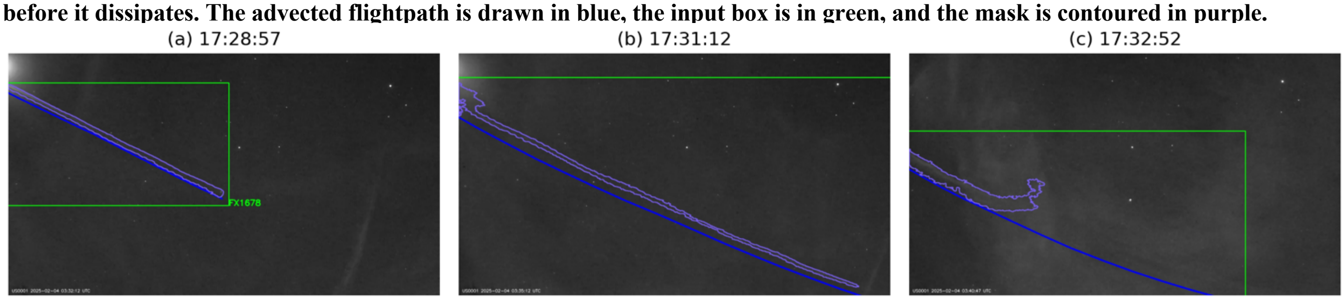

Figure S4: Overlaid masks from a contrail segmented successfully under nighttime conditions, showcasing the pipeline's robustness to varying conditions. The advected flightpath is drawn in blue, the input box is in green, and the mask is contoured in purple.

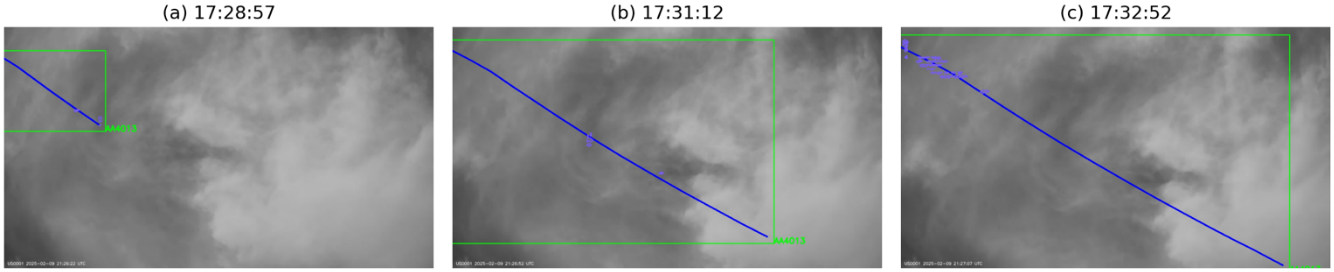

Figure S5: The overlaid masks from a true negative flight against a complicated background. Most frames of true negative flights have no mask output, but these masks highlight the contrast between the masks of negative and positive detections. The advected flightpath is drawn in blue, the input box is in green, and the mask is contoured in purple.

Figure S6: An example of a peripheral contrail, with an arrow indicating its location. These form near the edges or the corners of the frame and are sometimes missed due to the lack of separation from the boundary, and due to their visible short length.

Figure S7: An example of a missed contrail ,with arrows indicating its location, that was missed due to a combination of being partially obscured by cloud cover, visually faint, and against a complex background.

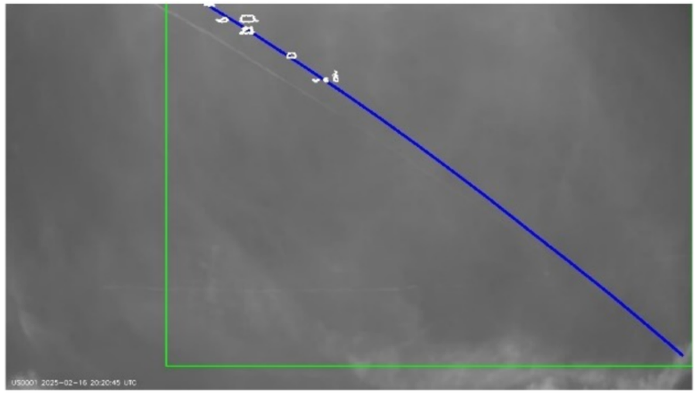

Figure S8: An example of a missed contrail due to SAM2 failing to segment out the contrail due to low local contrast, with the contrail appearing too faint. The advected flightpath is drawn in blue, the input box is in green, and the mask is contoured in white.

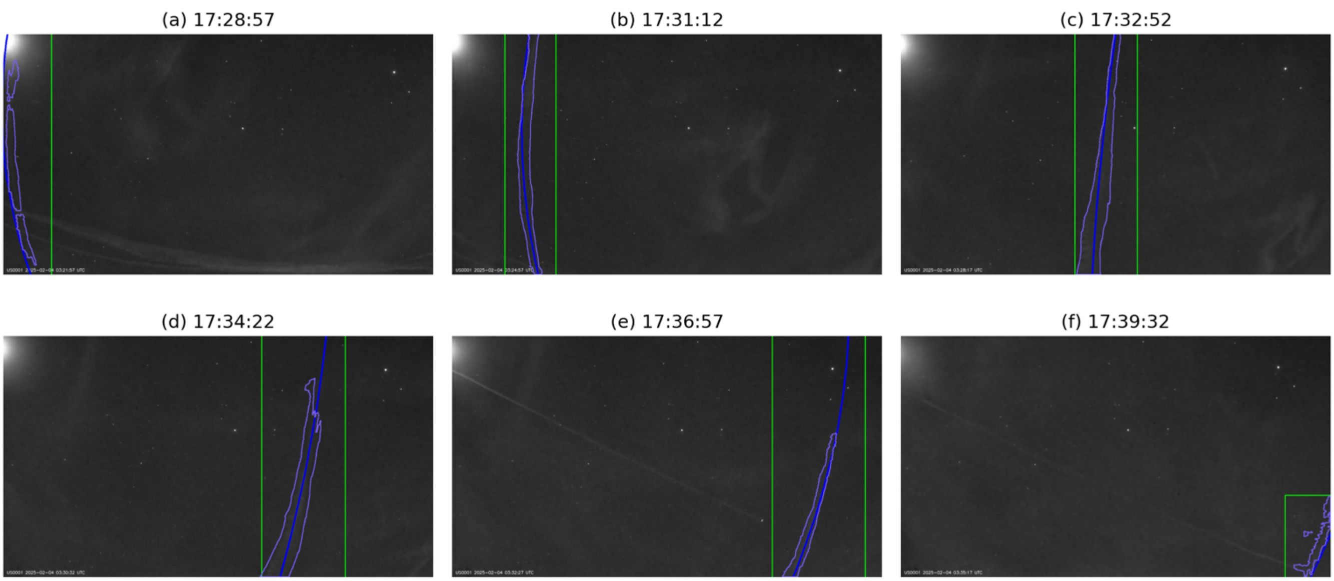

Figure S9 The overlaid masks from an advected contrail in nighttime conditions. The advected flightpath is drawn in blue, the input box is in green, and the mask is contoured in white.